Polyphenol Combination of Resveratrol and Ferulic Acid Ameliorates Cisplatin-Induced Renal Injury Via Regulation of the AMPK/p53/Akt Pathway

Bhargab Deka
Girijananda Chowdhury University
Trishna Das
drtrishnadas@gmail.com
Girijananda Chowdhury University
Dipankar Sahaa
Girijananda Chowdhury University
Bhrigu Kumar Das
Girijananda Chowdhury University
Smriti Rekha Chanda Das
Girijananda Chowdhury University
Rituparna Borah
Girijananda Chowdhury University
Tanmay Jit
Assam University
Mrinmoy Basak
Assam Down Town University

Research Article

Keywords: Resveratrol, Ferulic acid, Cisplatin, Nephrotoxicity, AMPK, p53

Posted Date: May 25th, 2026

DOI: https://doi.org/10.21203/rs.3.rs-9249818/v1

Additional Declarations: No competing interests reported.

Abstract

This study aimed to explore the nephroprotective effects of resveratrol (RSV) and ferulic acid (FA), both individually and in combination, against cisplatin-induced cytotoxicity in HEK-293 human renal epithelial cells, focusing on the adenosine monophosphate (AMP)-activated protein kinase/p53/Protein kinase B (AMPK/p53/Akt) signaling pathway, oxidative stress, and apoptosis. HEK-293 cells were treated with cisplatin (25 µg/mL) to induce nephrotoxicity *in-vitro*. RSV and FA were administered individually at 100 µg/mL and in combination at ratios of 1:1, 1:2, and 2:1. Cell viability was assessed using the MTT assay. Flow cytometry was used to measure the expression of AMPKα1, p53, Akt, B-cell lymphoma 2 (Bcl-2), Bcl-2-associated X protein (Bax), tumor necrosis factor-alpha (TNF-α), and active caspase-3. Lipid peroxidation was quantified by measuring the malondialdehyde (MDA) levels. Cisplatin decreased cell viability, activated the AMPK-p53 pathway, increased pro-apoptotic and inflammatory markers, and suppressed Akt and Bcl-2 expression. Co-treatment with RSV and FA (1:2) restored cell viability, downregulated AMPK–p53 activation, boosted Akt and Bcl-2, improved the Bax/Bcl-2 ratio, and reduced MDA and tumor necrosis factor-alpha levels, highlighting its antioxidant and anti-inflammatory effects. This study demonstrates that the co-administration of RSV and FA offers synergistic nephroprotection against cisplatin-induced damage in HEK-293 cells. This protective process operates through the modulation of the AMPK-p53 axis and activation of Akt, emphasizing the therapeutic potential of these compounds as adjuncts in cisplatin chemotherapy.

1. Introduction

Cisplatin is a widely prescribed platinum-based chemotherapeutic agent with established efficacy against a broad spectrum of solid tumors, including testicular, breast, ovarian, head and neck, and bladder cancers (Romani, 2022). Despite its clinical effectiveness, the therapeutic utility of cisplatin is markedly limited by dose-dependent nephrotoxicity, which affects approximately 20–30% of patients despite adequate hydration and supportive care protocols (Shahrahmani et al., 2025). Cisplatin-induced acute kidney injury (AKI) primarily arises from the preferential accumulation of cisplatin in renal tubular epithelial cells, leading to excessive oxidative stress, mitochondrial dysfunction, activation of apoptotic pathways, and a pronounced inflammatory response (Tang et al., 2023). Among the molecular regulators implicated in cisplatin-induced renal injury, the AMP-activated protein kinase (AMPK) pathway has emerged as a critical mediator of cellular stress response. AMPK functions as a central energy sensor and is activated under metabolic and oxidative stress conditions (Sharma et al., 2023). While AMPK activation is generally regarded as cytoprotective in multiple tissues, accumulating evidence suggests a paradoxical role in cisplatin-exposed renal tubular cells, where its upregulation has been linked to the amplification of apoptotic signalling through phosphorylation and activation of the tumor suppressor protein p53 (Jin et al., 2020; He et al., 2014). Activation of p53 subsequently promotes the transcription of pro-apoptotic proteins, including Bax, while concurrently suppressing anti-apoptotic factors, such as Bcl-2. This imbalance facilitates mitochondrial membrane permeabilization, caspase cascade activation, and irreversible commitment to programmed cell death (Hao et al., 2022). In contrast, the phosphoinositide 3-kinase (PI3K)/Akt pathway plays a pivotal role in maintaining cellular survival by

negatively regulating apoptotic processes, enhancing Bcl-2 expression, and functionally inhibiting p53 activity (Wang et al., 2024). However, cisplatin exposure suppresses Akt activation, exacerbating apoptotic damage and compromising renal cell viability (Huang et al., 2024). Accordingly, therapeutic modulation of these signalling axes, specifically the attenuation of AMPK/p53 activation coupled with the restoration of Akt signalling, represents a rational strategy for mitigating cisplatin-induced nephrotoxicity.

Natural plant-derived polyphenols have attracted considerable attention as potential cytoprotective agents because of their antioxidant, anti-inflammatory, and anti-apoptotic properties. Resveratrol (RSV), a stilbenoid polyphenol abundant in grapes and berries, is a well-characterized bioactive compound with protective effects against oxidative stress and inflammatory injury (Zhang et al., 2021). Notably, resveratrol has been reported to influence both AMPK and Akt signalling pathways, positioning it as a potential modulator of cellular energy homeostasis and survival mechanisms across diverse pathological contexts (Ren et al., 2025). Ferulic acid (FA), a hydroxycinnamic acid commonly found in cereals, fruits, and vegetables, exhibits potent antioxidant and free radical–scavenging activity and suppresses pro-inflammatory mediators while improving mitochondrial function (Kumar et al., 2025). Although resveratrol and ferulic acid have independently demonstrated nephroprotective effects in preclinical models, their combined therapeutic efficacy remains largely unexplored. The rationale for a combinatorial approach lies in the potential for synergistic cyto-protection through complementary mechanisms. RSV primarily enhances cell survival via Akt activation (Utpal et al., 2025), whereas FA attenuates lipid peroxidation and oxidative stress (Yang et al., 2025). Moreover, both compounds have been reported to modulate upstream regulators, including AMPK, providing a convergent pathway for the regulation of apoptotic signalling (He et al., 2016; Chen et al., 2022).

Hence, in this study, we investigated the nephroprotective potential of resveratrol and ferulic acid, individually and in combination, in HEK-293 cells exposed to cisplatin. This study focused on the AMPK-p53-Akt signalling axis as a central mechanism of cisplatin-induced cellular injury. It assessed downstream apoptotic markers (Bax, Bcl-2, and caspase-3), oxidative stress indices [malondialdehyde (MDA)], and inflammatory mediators (TNF-α). To ensure that the protective intervention did not compromise the anticancer efficacy of cisplatin, the RSV-FA combination was evaluated in MCF-7 breast cancer cells.

2. Materials and Methods

2.1 Chemicals and reagents

All chemicals and reagents used in this study were of analytical grade and procured from certified commercial suppliers. RSV and FA were obtained from Sigma-Aldrich Chemical Company (USA). Cisplatin was purchased from Sigma-Aldrich (USA) and used at a final concentration of 25 µg/mL to induce cytotoxicity. Cell culture reagents, including Dulbecco's modified Eagle's medium (DMEM), fetal bovine serum (FBS), 1× Dulbecco's phosphate-buffered saline (DPBS), 0.25% trypsin–EDTA solution, and

MTT reagent, were procured from MP Biomedicals (Germany). Cell culture-grade dimethyl sulfoxide (DMSO), used for formazan solubilization, was obtained from Merck (Darmstadt, Germany). Target-specific primary antibodies were used for flow cytometry analysis. Anti-human AMPKα1 rabbit IgG antibody (Cat. No. orb10076) and anti-human Akt rabbit IgG antibody were purchased from Biorbyt (Cambridge, UK). Anti-human TNF-α rabbit IgG antibody (Cat. No. E-AB-40015) was obtained from ElabScience (USA). Apoptotic markers were detected using an FITC-conjugated anti-Bax antibody (cat. No. orb2078817; Biorbyt) and PE-conjugated anti-Bcl-2 antibody (Cat. No. 340576; BD Biosciences), FITC-labelled anti-p53 antibody (Cat. No. 645803; BioLegend) and an FITC rabbit anti-active caspase-3 IgG antibody (Cat. No. 559341; BD Biosciences). FITC-conjugated goat anti-rabbit IgG secondary antibody (Cat. No. 554020) was obtained from BD Biosciences and used as required. The reagents used for cell fixation and permeabilization included 2% paraformaldehyde, 0.5% bovine serum albumin (BSA) prepared in phosphate-buffered saline, and 0.1% Triton X-100 in BSA solution, all sourced from HiMedia (India). Lipid peroxidation was assessed using a thiobarbituric acid (TBA)-based assay with reagents purchased from SRL Chemicals (India). The malondialdehyde (MDA) standard used for calibration was obtained from Merck (Darmstadt, Germany).

2.2 Cell culture conditions and instrumentation

Human embryonic kidney epithelial cells (HEK-293) were procured from the National Center for Cell Science (NCCS; Pune, India). Cells were maintained in Dulbecco's Modified Eagle Medium (DMEM) supplemented with 10% heat-inactivated FBS and cultured at 37°C in a humidified incubator under a 5% CO_2 atmosphere. Subculturing was performed when cultures reached approximately 70–80% confluence using 0.25% trypsin-EDTA solution. HEK-293 cells between passages 5 and 15 were used for all the experimental procedures. For routine expansion, cells were seeded in T-25 culture flasks and subsequently transferred to the appropriate culture plates or wells for downstream assays.

All experiments involving cell culture and flow cytometric analyses were conducted in accordance with standard biosafety level II (BSL-2) practices. Cell culture procedures were performed under aseptic conditions in a Class II A2 biological safety cabinet (Model BSC-1300IIA2-X; Biobase, China). Cells were maintained in a CO_2 incubator (Model ZOCR-1150B; Labwit, Australia) at 37°C under a humidified atmosphere containing 5% CO_2 and approximately 95% relative humidity. Cellular imaging and morphological assessments were performed using an XDFL series inverted microscope (Sunny Instruments, China). Absorbance measurements for the MTT assay were obtained using a BK-EL10A microplate reader (Biobase, China). Flow cytometric data were acquired on a Cytomics FC500 flow cytometer (Beckman Coulter, USA) and analysed using FlowJo X (version 10.0.7). Image analysis, where applicable, was performed using ImageJ (Fiji) software (version 1.53j).

2.3 Cell viability assay

The cytoprotective effects of resveratrol (RSV), ferulic acid (FA), and their combination were assessed using the MTT assay, as previously described (Gerlier and Thomasset, 1986). Briefly, HEK-293 cells were seeded into 96-well culture plates at 1×10^4 cells per well in 200 µL of complete culture medium and

allowed to adhere for 24 h before treatment. Following initial incubation, the cells were treated with RSV, FA, their respective combinations, or cisplatin for 48 h. RSV and FA were evaluated individually at 100 µg/mL and in combination at fixed total doses in ratios of 1:1, 1:2, and 2:1. Cisplatin was administered at 25 µg/mL to induce cytotoxicity. At the end of the treatment period, the culture medium was carefully removed and replaced with 200 µL of fresh medium containing MTT reagent (0.5 mg/mL), and the culture was incubated for an additional 3 h at 37°C. The resulting formazan crystals were solubilized by adding 100 µL dimethyl sulfoxide (DMSO) per well. Absorbance was measured at 570 nm with a reference wavelength of 630 nm using a microplate reader. Cell viability was expressed as a percentage relative to that of untreated control cells (Mosmann, 1983).

2.4 Flow cytometric evaluation of intracellular signaling proteins (AMPKα1, Akt), inflammatory marker (TNF-α), apoptotic marker (Bax, Bcl-2, Caspase-3), and p53

Flow cytometry was used to evaluate the intracellular expression of key signalling and apoptotic markers, including AMPKα1, Akt, TNF-α, Bax, Bcl-2, active caspase-3, and p53. HEK-293 cells were seeded into 6-well culture plates at a density of 3×10^5 cells per well and allowed to adhere for 24 h. The cells were subsequently treated with the respective test compounds and cisplatin for an additional 24 h. Following treatment, the cells were harvested by trypsinization using 200 µL of trypsin-EDTA, neutralized with complete culture medium, and centrifuged at 300 × g for 5 min. The resulting cell pellets were washed twice with phosphate-buffered saline (PBS), fixed with 2% paraformaldehyde for 20 min at room temperature, and permeabilized using 0.1% Triton X-100 prepared in 0.5% bovine serum albumin (BSA) for 10 min at room temperature. After additional washing with BSA–PBS, the cells were incubated in 500 µL of 0.5% BSA–PBS containing 20 µL of the appropriate primary antibody. Antibody staining was performed for 30 min at room temperature, in the dark. Following incubation, the cells were washed to remove unbound antibodies, and fluorophore-conjugated secondary antibodies (FITC-labelled) were added where required, followed by a further 30 min incubation in the dark. Finally, the cells were resuspended in PBS and analyzed using flow cytometry. Data acquisition and analysis were performed using FlowJo software, and the results were expressed as the geometric mean fluorescence intensity (MFI) and the percentage of high-expressing cells for each marker (Faiao-Flores et al., 2013; Das et al., 2021).

2.5 MDA assay for lipid peroxidation

Oxidative stress was evaluated by quantifying malondialdehyde (MDA) levels, a well-established marker of lipid peroxidation, using a thiobarbituric acid reactive substances (TBARS) assay. Following 24 h of drug treatment, HEK-293 cells were lysed in 0.5 mL of a solvent containing 50% glacial acetic acid supplemented with 0.01% butylated hydroxytoluene (BHT) to prevent ex vivo lipid oxidation. The resulting cell lysates were centrifuged at 10,000 × g for 10 min, and the supernatants were collected for further analysis. An aliquot of 0.5 mL of the supernatant was mixed with an equal volume (0.5 mL) of freshly prepared thio-barbituric acid (TBA) reagent and incubated in a boiling water bath at 95°C for 1 h to allow chromogen formation. After cooling to room temperature and centrifugation to remove precipitates, 200 µL of the clarified supernatant was transferred to a 96-well microplate. The absorbance was measured at

532 nm using a microplate reader. MDA concentrations were calculated from a standard calibration curve generated using known MDA concentrations ranging from 3.125 to 50 μM (Yagi, 1998; Zeb and Ullah, 2016).

2.6 Statistical Analysis

All experimental data are presented as mean ± standard error of the mean (SEM) derived from at least three independent experiments per group. Statistical analyses were performed using GraphPad Prism software (version 9.0; GraphPad Software). Comparisons among multiple experimental groups were conducted using one-way analysis of variance (ANOVA), followed by Bonferroni's post hoc test for multiple comparisons, with $p < 0.05$ as the significance threshold.

3. Results

3.1 Effect of RSV and FA on cisplatin-induced cytotoxicity in HEK-293 cells

Treatment with RSV or FA alone, up to 200 μg/mL, showed no observable cytotoxic effects, validating their biocompatibility at the tested concentrations (Figs. 1 and 2). Cisplatin at 25 μg/mL markedly reduced HEK-293 cell viability, confirming successful induction of cytotoxicity. Notably, co-treatment with RSV and FA at various ratios (1:1, 1:2, and 2:1) significantly improved cell viability in the presence of cisplatin (Fig. 3). Among these, the 1:2 combination (RSV: FA = 33.3 μg/mL:66.7 μg/mL) produced the most substantial cytoprotective effect, restoring viability to a level significantly higher than that observed with cisplatin treatment alone ($p < 0.001$).

3.2 RSV-FA co-treatment modulates AMPKα1 expression

Flow cytometric analysis revealed that cisplatin treatment elevated the expression of AMPKα1 in HEK-293 cells, suggesting the activation of the cellular energy stress response (Fig. 4). However, co-treatment with the RSV-FA 1:2 combination significantly attenuated AMPKα1 expression compared to the cisplatin-only group ($p < 0.01$). This modulation of AMPK activity indicates the potential regulatory effects of RSV and FA on upstream stress signaling pathways, contributing to cell injury.

3.3 RSV-FA co-treatment suppressed p53 phosphorylation

Consistent with AMPK activation, cisplatin-treated cells exhibited a pronounced increase in phosphorylated p53 expression, as indicated by a substantial rightward shift in fluorescence intensity. The RSV-FA combination significantly reduced p53 phosphorylation levels ($p < 0.001$), indicating that the cytoprotective effects were partially mediated by suppression of the AMPK-p53 axis (Fig. 5). This reduction likely contributes to decreased downstream apoptotic signaling.

3.4 RSV-FA co-treatment restores Akt expression

Cisplatin exposure markedly suppressed Akt expression, confirming inhibition of cell-survival pathways. Interestingly, RSV-FA treatment reversed this effect, resulting in a significant increase in Akt expression compared with cisplatin treatment alone ($p < 0.001$) (Fig. 6). This restoration of Akt suggests that the RSV-FA combination promotes pro-survival signaling in cisplatin-injured cells, supporting its protective effect.

3.5 RSV-FA alters Bax and Bcl-2 expression favorably

Cisplatin significantly increased pro-apoptotic Bax expression and decreased anti-apoptotic Bcl-2 levels compared with the control ($p < 0.01$). RSV–FA co-treatment significantly downregulated Bax ($p < 0.01$ vs. cisplatin) and upregulated Bcl-2 ($p < 0.05$ vs. cisplatin), suggesting attenuation of intrinsic apoptotic signaling (Figs. 7 and 8).

3.6 Effect of RSA-FA co-treatment on TNF-α expression

Co-treatment did not significantly alter TNF-α expression in cisplatin-treated cells relative to controls, indicating minimal involvement of this cytokine in the observed nephroprotective effect (Fig. 9).

3.7 Cell Viability and Caspase-3 activation in MCF-7 cells

To evaluate whether RSV-FA co-treatment interferes with the anticancer efficacy of cisplatin, MCF-7 breast cancer cells were analyzed for cell viability and caspase-3 expression levels. Cisplatin treatment alone strongly activates caspase-3. Notably, co-treatment with RSV-FA enhanced caspase-3 activation and reduced cell viability, indicating the potentiation of cisplatin’s apoptotic effect in cancer cells (Fig. 10). This finding confirmed that the combination does not diminish and may even augment the cytotoxicity of cisplatin in malignant cells.

3.8 RSV-FA reduces cisplatin-induced lipid peroxidation

Cisplatin significantly increased malondialdehyde (MDA) levels in HEK-293 cells ($p < 0.001$ vs. control), indicating increased oxidative stress. Co-treatment with RSV-FA significantly reduced MDA levels compared with cisplatin alone ($p < 0.001$), confirming the combination's antioxidant potential (Fig. 11).

4. Discussion

Cisplatin remains a cornerstone of chemotherapy for various solid tumors; however, its clinical application is constrained by dose-dependent nephrotoxicity, which affects approximately 30% of patients (Oliveira et al., 2024). This toxicity predominantly targets the renal proximal tubules, where cisplatin accumulates, triggering a cascade of cellular damage through DNA damage, oxidative stress, and inflammation (Firdous et al., 2025). The urgent need for nephroprotective strategies that preserve cisplatin's anticancer efficacy has driven research into the molecular mechanisms underlying its toxicity. This study investigated the role of the AMP-activated protein kinase (AMPK)-p53 signaling axis in

cisplatin-induced acute kidney injury (AKI). It evaluated the nephroprotective potential of co-treatment with RSV and FA.

The AMPK-p53 signaling pathway is a critical mediator of cisplatin-induced renal injury. AMPK, a master regulator of cellular energy homeostasis, is activated in response to cisplatin-induced stress in renal tubular epithelial cells, as evidenced by increased phosphorylation at Thr172 (Jin et al., 2020). This activation promotes the phosphorylation of p53, a tumor suppressor protein that orchestrates cellular responses to stress, including apoptosis and cell cycle arrest (Jiang and Dong, 2008).

Phosphorylated p53 upregulates pro-apoptotic genes, such as Bax, leading to mitochondrial dysfunction, caspase activation, and tubular cell apoptosis (Wei et al., 2007). In addition, p53 contributes to inflammatory responses, further exacerbating renal damage (Overstreet et al., 2022). These findings align with previous reports demonstrating that cisplatin-induced AMPK activation drives p53-mediated apoptosis in renal cells, contributing significantly to AKI (Ju et al., 2021). Thus, targeting the AMPK-p53 axis may be a promising strategy for mitigating cisplatin-induced nephrotoxicity. RSV and FA are polyphenolic compounds with well-established antioxidant, anti-inflammatory, and cytoprotective properties (Peng et al., 2024; Khan et al., 2024). Resveratrol modulates AMPK activity in various disease models and often exerts context-dependent effects (Park et al., 2007). Similarly, ferulic acid is recognized for its ability to counteract oxidative stress and inflammation (Mancuso and Santangelo, 2014). The synergistic potential of these compounds prompted us to evaluate their combined therapeutic effects in the present study. Using HEK-293 cells, we demonstrated that cisplatin treatment significantly reduced cell viability, increased AMPK and p53 phosphorylation, upregulated pro-apoptotic Bax and active caspase-3 levels, and decreased anti-apoptotic Bcl-2 and Akt expression levels. Co-treatment with RSV and FA, particularly at a 1:2 ratio (33.3 µg/mL RSV: 66.7 µg/mL FA), effectively reversed these effects, restored cell viability, and attenuated the levels of apoptotic markers. The observed downregulation of AMPK and p53 phosphorylation by RSV-FA co-treatment is a key finding, suggesting that these compounds interrupt the detrimental signaling cascade initiated by cisplatin. The upregulation of Akt, a critical survival kinase, further supports cellular resilience to cisplatin-induced oxidative stress.

Additionally, the RSV-FA combination reduced lipid peroxidation, as measured by malondialdehyde (MDA) levels, highlighting its antioxidant capacity. These results are consistent with those of previous studies demonstrating the protective effects of polyphenolic compounds against oxidative stress and apoptosis in various models of kidney injury. The nephroprotective effects of RSV and FA co-treatment are attributable to their multifaceted modulation of the AMPK-p53 axis, oxidative stress, and apoptosis. By suppressing AMPK activation, RSV-FA reduced p53 phosphorylation, thereby inhibiting the transcription of pro-apoptotic genes and mitigating tubular-cell death. The upregulation of Akt likely enhances cell-survival pathways, thereby counteracting the pro-apoptotic effects of cisplatin. The reduction in MDA levels underscores the antioxidant properties of RSV and FA, which neutralize reactive oxygen species (ROS) generated by cisplatin, a well-documented contributor to nephrotoxicity [14].

These findings suggest that RSV and FA act synergistically to target multiple pathogenic mechanisms, offering a comprehensive protective strategy.

Notably, the lack of a significant change in TNF-α expression following RSV-FA co-treatment is intriguing. While cisplatin increased TNF-α levels, consistent with its proinflammatory role, the RSV-FA combination did not alter cytokine expression. This suggests that the anti-inflammatory effects of RSV-FA may be mediated through alternative pathways, such as NF-κB or IL-1β inhibition, which are known to contribute to cisplatin-induced inflammation (Ozkok and Edelstein, 2014). The precise mechanisms underlying the selective effects on inflammatory markers warrant further investigation.

A critical aspect of this study was the preservation of anticancer efficacy of cisplatin. In MCF-7 breast cancer cells, RSV-FA cotreatment enhanced the cytotoxicity of cisplatin, increased caspase-3 activation, and reduced cell viability. This dual action of protecting renal cells while potentiating cancer cell death positions RSV-FA as a promising adjunctive therapy for cisplatin-based chemotherapy. The synergistic 1:2 ratio of RSV to FA highlights the importance of optimizing combination therapy to maximize its therapeutic benefits. The role of AMPK in cisplatin-induced nephrotoxicity remains a subject of debate, with conflicting results. Our findings align with previous studies, demonstrating that AMPK activation contributes to cisplatin-induced apoptosis by phosphorylating p53. Inhibition of AMPK with compound C has been shown to reduce p53 phosphorylation, Bax expression, and caspase-3 activation, protecting against renal injury in both *in vitro* and *in vivo* models (Jin et al., 2020; Ju et al., 2021). These studies support the notion that excessive or prolonged AMPK activation in the context of cisplatin toxicity is detrimental, driving apoptotic and inflammatory pathways in the renal cells. Conversely, other studies suggest that AMPK activation can be protective in kidney injury models, often through induction of autophagy (Hu et al., 2021). Canagliflozin, an AMPK activator, protects against cisplatin-induced AKI by promoting autophagy in renal proximal tubule cells (Park et al., 2022). Similarly, metformin and AICAR, both AMPK activators, have demonstrated reno-protective effects in specific contexts (Ravindran et al., 2017; Xu et al., 2024). These discrepancies may arise from differences in the experimental models, cell types, and specific pathways modulated by AMPK. In cisplatin-induced nephrotoxicity, the balance between AMPK's pro-survival and pro-apoptotic roles may depend on the duration and intensity of its activation and the cellular context. Our study suggests that in HEK-293 cells, the pro-apoptotic effects of AMPK predominate; thus, inhibition of AMPK by RSV-FA is beneficial.

5. Limitations and future directions

The present study demonstrates that RSV and FA, particularly in combination, attenuate cisplatin-induced cytotoxicity in renal epithelial cells by modulating the AMPK–p53–Akt signalling axis and downstream apoptotic mediators. The observed restoration of Akt activity, concomitant suppression of AMPK-p53 signalling, and normalization of the Bax/Bcl-2 balance collectively suggest a shift toward a pro-survival cellular phenotype. These findings are consistent with previous reports implicating dysregulated energy sensing and survival signalling in cisplatin-induced renal injury and further support the therapeutic relevance of targeting these pathways using bioactive polyphenols. Notably, the absence

of protective interference with cisplatin cytotoxicity in MCF-7 cells underscores the potential selectivity of the RSV-FA combination for renal protection without compromising anticancer efficacy. However, this observation warrants validation in additional tumor models.

Despite these promising mechanistic insights, several limitations of this study should be acknowledged. First, although HEK-293 cells are widely used to model renal epithelial injury, they do not fully recapitulate the cellular heterogeneity and microenvironmental complexity of the kidney *in-vivo*. Accordingly, confirmation of these findings in primary renal tubular epithelial cells and established animal models of cisplatin-induced acute kidney injury (AKI) is necessary to strengthen their translational relevance. Second, although the present data implicate AMPK modulation as a central event, the precise upstream regulatory mechanisms by which RSV and FA influence AMPK activity remain to be elucidated. The lack of significant modulation of TNF-α expression further suggests that the anti-inflammatory effects of RSV-FA may involve alternative, TNF-independent pathways in cells. In addition, although the 1:2 RSV-FA ratio was the most effective under in vitro conditions, extrapolation to clinical applications requires comprehensive pharmacokinetic and pharmacodynamic evaluations. Finally, exploring additional signalling cascades implicated in cisplatin nephrotoxicity, including the MAPK and NF-κB pathways, would provide a more integrated understanding of the protective mechanisms and help delineate the broader therapeutic potential of this combinatorial strategy.

6. Conclusion

The present study demonstrates that combined treatment with RSV and FA attenuates cisplatin-induced cytotoxicity in renal epithelial cells by coordinating the modulation of the AMPK–p53 signaling axis and downstream apoptotic pathways. The RSV–FA combination, particularly at a 1:2 ratio, restored cell viability, suppressed AMPK and p53 activation, reduced Bax and caspase-3 expression, and enhanced Akt and Bcl-2 signaling, thereby favoring a pro-survival response. The concomitant reduction in lipid peroxidation further supports the contribution of antioxidant mechanisms to the observed nephroprotective effects. Significantly, RSV-FA co-treatment did not compromise the anticancer activity of cisplatin in MCF-7 breast cancer cells, suggesting a degree of cellular selectivity for its protective action. Nevertheless, the absence of significant modulation of TNF-α expression and the context-dependent role of AMPK in renal injury highlight the need for further mechanistic investigations. Validation of these findings in vivo, together with pharmacokinetic and pharmacodynamic evaluations, will be essential to determine their translational relevance. Collectively, this study adds to the growing evidence that targeted modulation of AMPK-p53 signaling may represent a viable strategy for improving the renal safety profile of cisplatin-based chemotherapy.

Declarations

Consent for publications

Not applicable.

Availability of data and materials

Not applicable.

Competing interests

The authors state no conflict of interest.

Funding

We declare that there is no funding source for the above article.

Authors' contributions

BD and BKD designed this study. BD performed the experiments, analyzed the data, and drafted the manuscript. BKD coordinated the laboratory work and contributed to data interpretation and manuscript revision. TD supervised the work and critically revised the manuscript. DS assisted with the experiments, data processing, and statistical analysis. All the authors have read and approved the final manuscript.

Acknowledgement

The authors acknowledge Cell Kraft Biotech Pvt. Ltd., Bangalore, Karnataka, India, for providing the necessary facilities to conduct this research. The authors also acknowledge the School of Pharmaceutical Sciences, Girijananda Chowdhury University, including its DST-FIST Programme (FIST Programme-2021) supported laboratory facilities, for their infrastructural support during the course of this work. The DST-FIST support is acknowledged with Reference No. **SR/FST/COLLEGE-/2021/1172 (TPN-69342)**.

References

1. Chen T, Niu L, Wang L, Zhou Q, Zhao X, Lai S, He X, He H, He M (2022) Ferulic acid protects renal tubular epithelial cells against anoxia/reoxygenation injury mediated by AMPKα1. Free Radic Res 56(2):173–184
2. Das BK, Knott RM, Gadad PC (2021) Metformin and asarone inhibit HepG2 cell proliferation in a high glucose environment by regulating AMPK and Akt signaling pathway. Future J Pharm Sci 7(1):43
3. Faiao-Flores F, Coelho PRP, Arruda-Neto T, Maria-Engler JD, Tiago SS, Capelozzi M, Giorgi VL, R. R., Maria DA (2013) Apoptosis through Bcl-2/Bax and cleaved caspase up-regulation in melanoma treated by boron neutron capture therapy. PLoS ONE, 8(3), e59639
4. Firdous SM, Mahanta S, Malik S (2025) Underpinning the role of natural products against cisplatin-induced nephrotoxicity in rodent models. Med Chem Res 34:2378–2397
5. Gerlier D, Thomasset N (1986) Use of MTT colorimetric assay to measure cell activation. J Immunol Methods 94(1–2):57–63

6. Hao Q, Chen J, Lu H, Zhou X (2022) The ARTS of p53-dependent mitochondrial apoptosis. J Mol Cell Biol 14(10):mjac074
7. He G, Zhang Y-W, Lee J-H, Zeng SX, Wang YV, Luo Z, Dong XC, Viollet B, Wahl GM, Lu H (2014) AMP-activated protein kinase induces p53 by phosphorylating MDMX and inhibiting its activity. Mol Cell Biol 34(2):148–157
8. He T, Xiong J, Nie L, Yu Y, Guan X, Xu X, Xiao T, Yang K, Liu L, Zhang D (2016) Resveratrol inhibits renal interstitial fibrosis in diabetic nephropathy by regulating AMPK/NOX4/ROS pathway. J Mol Med 94:1359–1371
9. Hu X, Ma Z, Wen L, Li S, Dong Z (2021) Autophagy in cisplatin nephrotoxicity during cancer therapy. Cancers 13(22):5618
10. Huang T-L, Jiang W-J, Zhou Z, Shi T-F, Yu M, Yu M, Si J-Q, Wang Y-P, Li L (2024) Quercetin attenuates cisplatin-induced mitochondrial apoptosis via PI3K/Akt mediated inhibition of oxidative stress in pericytes and improves the blood labyrinth barrier permeability. Chemico-Biol Interact 393:110939
11. Jiang M, Dong Z (2008) Regulation and pathological role of p53 in cisplatin nephrotoxicity. J Pharmacol Exp Ther 327(2):300–307
12. Jin X, An C, Jiao B, Safirstein RL, Wang Y (2020) AMP-activated protein kinase contributes to cisplatin-induced renal epithelial cell apoptosis and acute kidney injury. Am J Physiology-Renal Physiol 319(6):F1073–F1080
13. Ju SM, Bae J, Jeon B-H (2021) AMP-activated protein kinase contributes to ROS-mediated p53 activation in cisplatin-induced nephrotoxicity. Eur Rev Med Pharmacol Sci 25(21):6691–6700
14. Khan KA, Saleem MH, Afzal S, Hussain I, Ameen F, Fahad S (2024) Ferulic acid: Therapeutic potential due to its antioxidant properties, role in plant growth, and stress tolerance. Plant Growth Regul 104(3):1329–1353
15. Kumar M, Kaushik D, Shubham S, Kumar A, Kumar V, Oz E, Brennan C, Zeng M, Proestos C, Çadırcı K (2025) Ferulic acid: extraction, estimation, bioactivity and applications for human health and food. J Sci Food Agric 105(8):4168–4177
16. Mancuso C, Santangelo R (2014) Ferulic acid: pharmacological and toxicological aspects. Food Chem Toxicol 65:185–195
17. Mosmann T (1983) Rapid colorimetric assay for cellular growth and survival: application to proliferation and cytotoxicity assays. Immunol. Meth. 65: 55–63. *Wiley, New York, NY, USA*, 13, 262
18. Oliveira CA, Mercês ÉaB, Portela FS, Malheiro LFL, Silva HBL, De Benedictis LM, De Benedictis JM, Silva CC D. Á., Santos E, A. C. L., Rosa DP (2024) An integrated view of cisplatin-induced nephrotoxicity, hepatotoxicity, and cardiotoxicity: characteristics, common molecular mechanisms, and current clinical management. *Clinical and Experimental Nephrology*, 28(8), 711–727
19. Overstreet JM, Gifford CC, Tang J, Higgins PJ, Samarakoon R (2022) Emerging role of tumor suppressor p53 in acute and chronic kidney diseases. Cell Mol Life Sci 79(9):474
20. Ozkok A, Edelstein CL (2014) Pathophysiology of cisplatin-induced acute kidney injury. Biomed Res Int 2014(1):967826

21. Park CE, Kim M-J, Lee JH, Min B-I, Bae H, Choe W, Kim S-S, Ha J (2007) Resveratrol stimulates glucose transport in C2C12 myotubes by activating AMP-activated protein kinase. Exp Mol Med 39(2):222–229
22. Park CH, Lee B, Han M, Rhee WJ, Kwak MS, Yoo T-H, Shin J-S (2022) Canagliflozin protects against cisplatin-induced acute kidney injury by AMPK-mediated autophagy in renal proximal tubular cells. Cell death discovery 8(1):12
23. Peng L, Hu X-Z, Liu Z-Q, Liu W-K, Huang Q, Wen Y (2024) Therapeutic potential of resveratrol through ferroptosis modulation: insights and future directions in disease therapeutics. Front Pharmacol 15:1473939
24. Ravindran S, Kuruvilla V, Wilbur K, Munusamy S (2017) Nephroprotective effects of metformin in diabetic nephropathy. J Cell Physiol 232(4):731–742
25. Ren ZQ, Zheng SY, Sun Z, Luo Y, Wang YT, Yi P, Li YS, Huang C, Xiao WF (2025) Resveratrol: Molecular Mechanisms, Health Benefits, and Potential Adverse Effects. MedComm, 6(6), e70252
26. Romani AM (2022) Cisplatin in cancer treatment. Biochem Pharmacol 206:115323
27. Shahrahmani F, Badamchizadeh S, Kaihani F, Alavi-Moghadam S, Keshtkari S, Rezaei-Tavirani M, Arjmand R, Larijani B, Arjmand B (2025) Platinum-based chemotherapies-induced nephrotoxicity: mechanisms, potential treatments, and management. Int Urol Nephrol 57(5):1563–1583
28. Sharma A, Anand SK, Singh N, Dwivedi UN, Kakkar P (2023) AMP-activated protein kinase: An energy sensor and survival mechanism in the reinstatement of metabolic homeostasis. Exp Cell Res 428(1):113614
29. Tang C, Livingston MJ, Safirstein R, Dong Z (2023) Cisplatin nephrotoxicity: new insights and therapeutic implications. Nat Rev Nephrol 19(1):53–72
30. Utpal BK, Mokhfi FZ, Zehravi M, Sweilam SH, Gupta JK, Kareemulla S, Rao AA, Kumar VV, Krosuri P, Prasad D (2025) Resveratrol: A Natural Compound Targeting the PI3K/Akt/mTOR Pathway in Neurological Diseases. Mol Neurobiol 62(5):5579–5608
31. Wang H, Gao L, Zhao C, Fang F, Liu J, Wang Z, Zhong Y, Wang X (2024) The role of PI3K/Akt signaling pathway in chronic kidney disease. Int Urol Nephrol 56(8):2623–2633
32. Wei Q, Dong G, Yang T, Megyesi J, Price PM, Dong Z (2007) Activation and involvement of p53 in cisplatin-induced nephrotoxicity. Am J Physiology-Renal Physiol 293(4):F1282–F1291
33. Xu W, Zhu Y, Wang S, Liu J, Li H (2024) From adipose to ailing kidneys: the role of lipid metabolism in obesity-related chronic kidney disease. Antioxidants 13(12):1540
34. Yagi K (1998) Simple procedure for specific assay of lipid hydroperoxides in serum or plasma. Methods in molecular biology, vol 108. Clifton, pp 107–110
35. Yang G, Hu N, Gao J, Li X, Zhang B, Ma K (2025) Ferulic Acid Combines with Ascorbic Acid to Target MMP9 to Attenuate Cisplatin-Induced Ototoxicity Through the p38MAPK Signaling Pathway. Antioxidants 14(6):619

36. Zeb A, Ullah F (2016) A simple spectrophotometric method for the determination of thiobarbituric acid reactive substances in fried fast foods. J Anal methods Chem 2016(1):9412767
37. Zhang L-X, Li C-X, Kakar MU, Khan MS, Wu P-F, Amir RM, Dai D-F, Naveed M, Li Q-Y, Saeed M (2021) Resveratrol (RV): A pharmacological review and call for further research. Biomed Pharmacother 143:112164

Figures

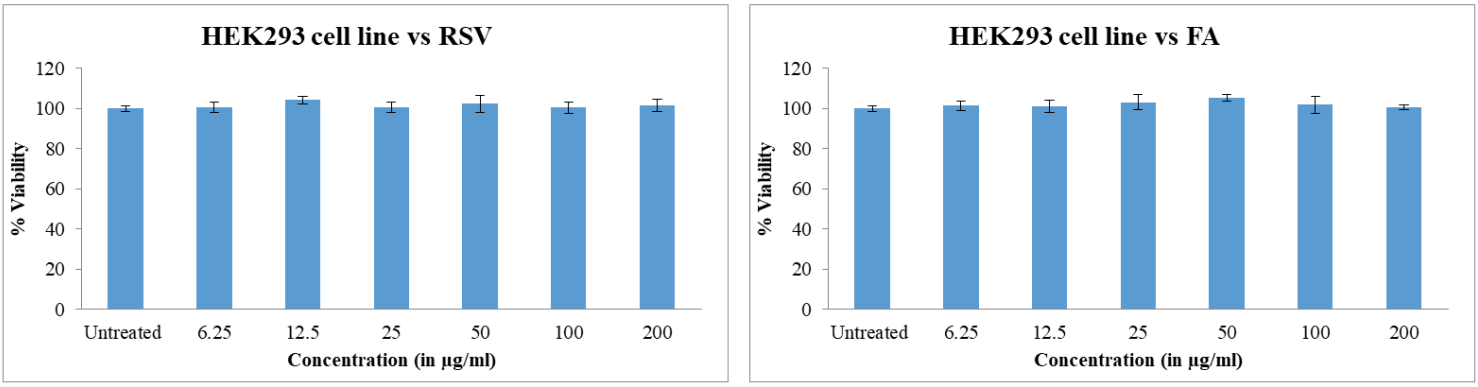

Figure 1

Cytotoxicity evaluation of RSV and FA in HEK-293 cells. HEK-293 cells were treated with increasing concentrations of RSV (left panel) and FA (right panel), ranging from 6.25 to 200 µg/mL, for 48 h. Cell viability was assessed using the MTT assay. Neither compound exhibited significant cytotoxicity across the tested concentration range compared to the untreated control, indicating biocompatibility with HEK-293 cells.

Abbreviations: RSV, Resveratrol; FA, Ferulic acid.

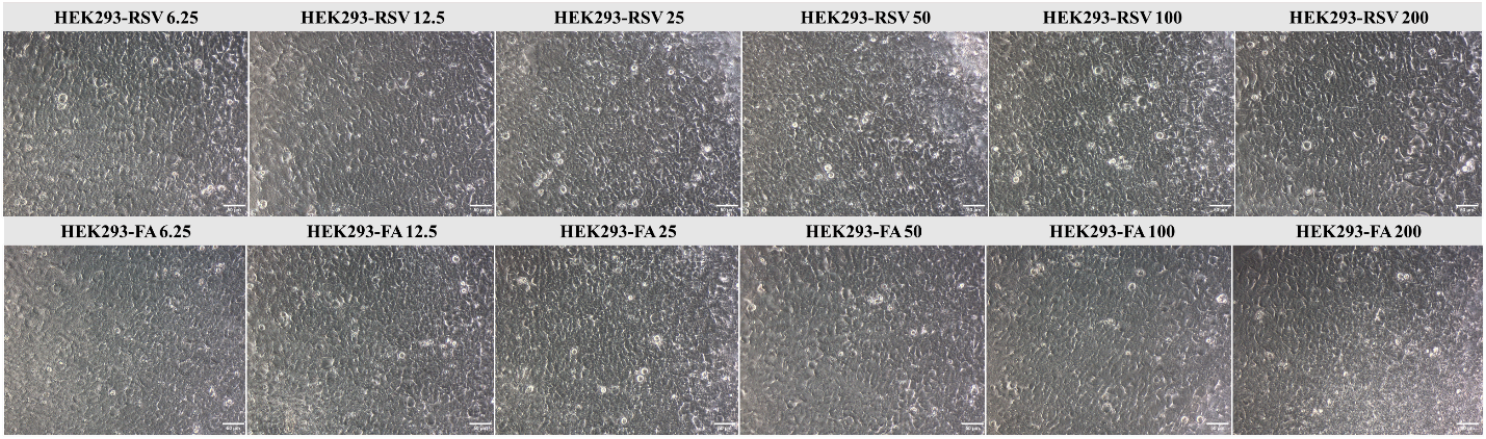

Figure 2

Normal morphology of the HEK293 cells treated with different concentrations ranging from 6.25 to 200 µg/mL of RSV and FA.

Abbreviations: RSV, Resveratrol; FA, Ferulic acid.

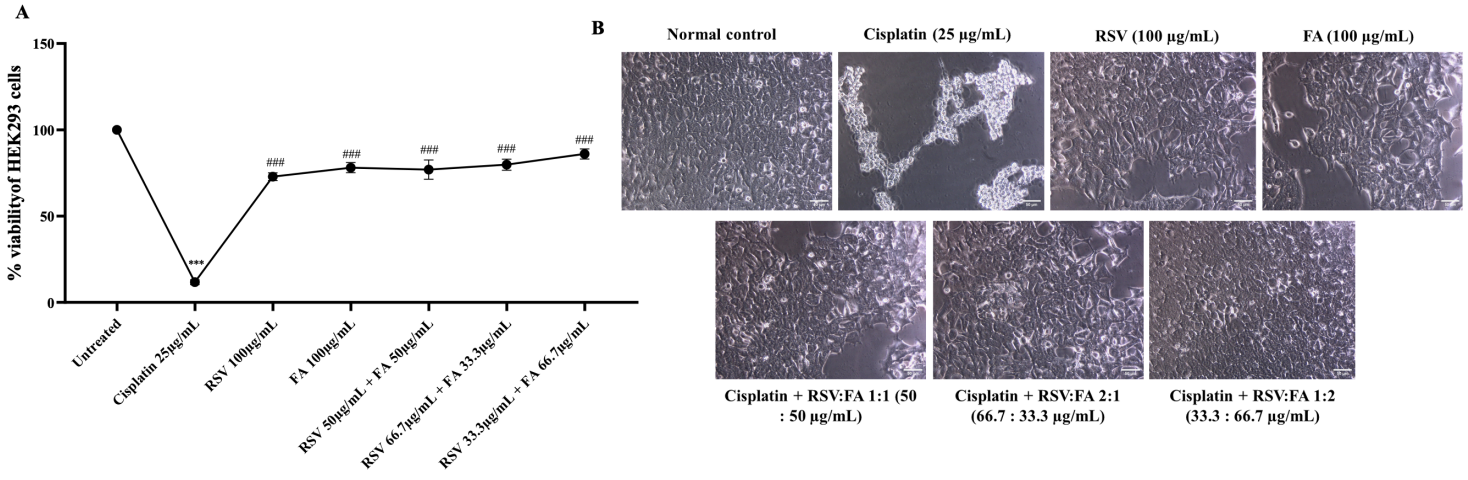

Figure 3

(A) Cells were treated with cisplatin, resveratrol (RSV), and ferulic acid (FA) at different concentrations and ratios for 48 h. Cell viability was assessed using the MTT assay. Values represent mean ± SEM of an experiment performed in triplicate; one-way ANOVA followed by Bonferroni test, where $^{***}p < 0.001$ compared to the untreated group, and $^{###}p < 0.001$ compared to the cisplatin group. **(B)** Cell morphology of HEK293 cells treated with different concentrations and ratios of cisplatin, resveratrol (RSV), and ferulic acid (FA). The bar scale is 50 µm.

Abbreviations: RSV, Resveratrol; FA, Ferulic acid.

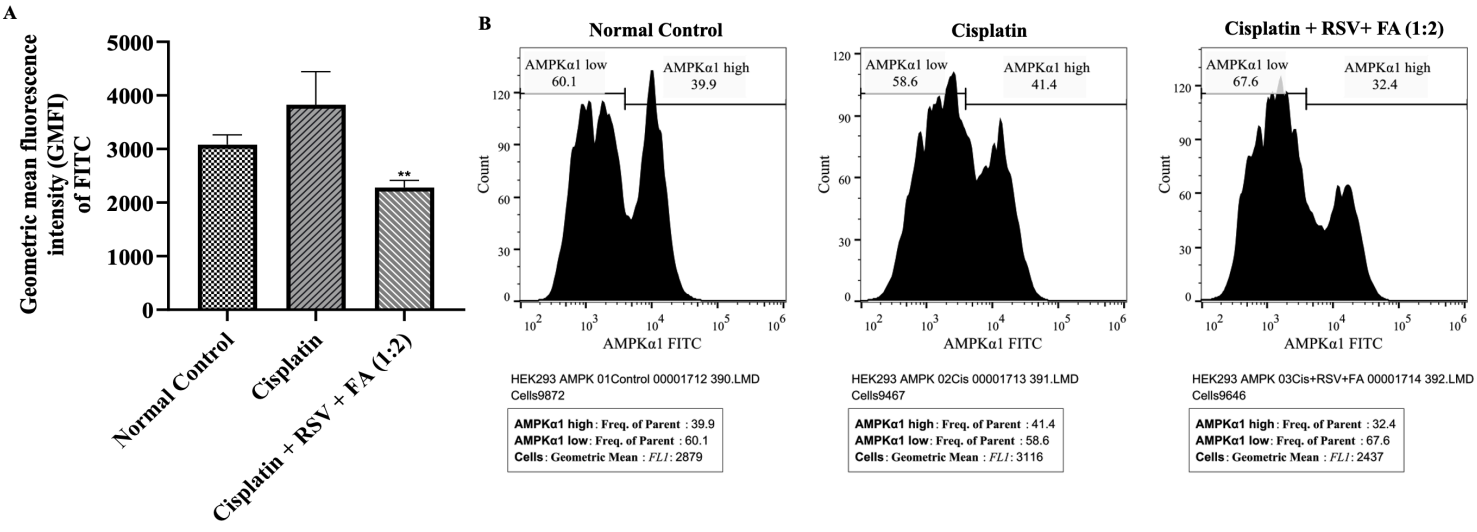

Figure 4

(A) The bar diagram represents the geometric mean fluorescence intensity (GMFI) of AMPKα1 in the different experimental groups. Values represent mean ± SEM of experiments performed in triplicate; one-way ANOVA followed by Bonferroni test, where $^{**}p < 0.01$ compared to the cisplatin group. **(B)** Flow cytometry histograms showing AMPKα1 expression in HEK 293 cells across the different experimental groups.

Abbreviations: RSV, Resveratrol; FA, Ferulic acid.

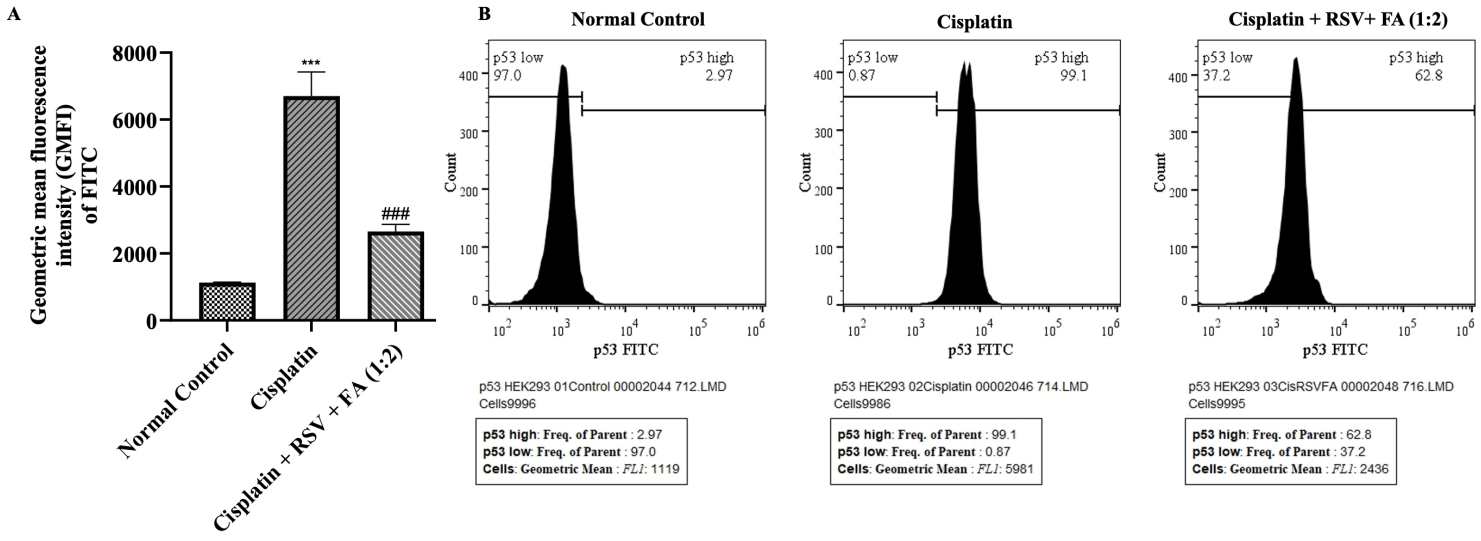

Figure 5

(A) The bar diagram represents the geometric mean fluorescence intensity (GMFI) of p53 in the different experimental groups. Values represent mean ± SEM of experiments performed in triplicate; one-way ANOVA followed by Bonferroni test, where $^{***}p < 0.001$ compared to the normal control group and $^{###}p < 0.001$ compared to the cisplatin group. **(B)** Flow cytometry histograms showing p53 expression in HEK 293 cells across the different experimental groups.

Abbreviations: RSV, Resveratrol; FA, Ferulic acid.

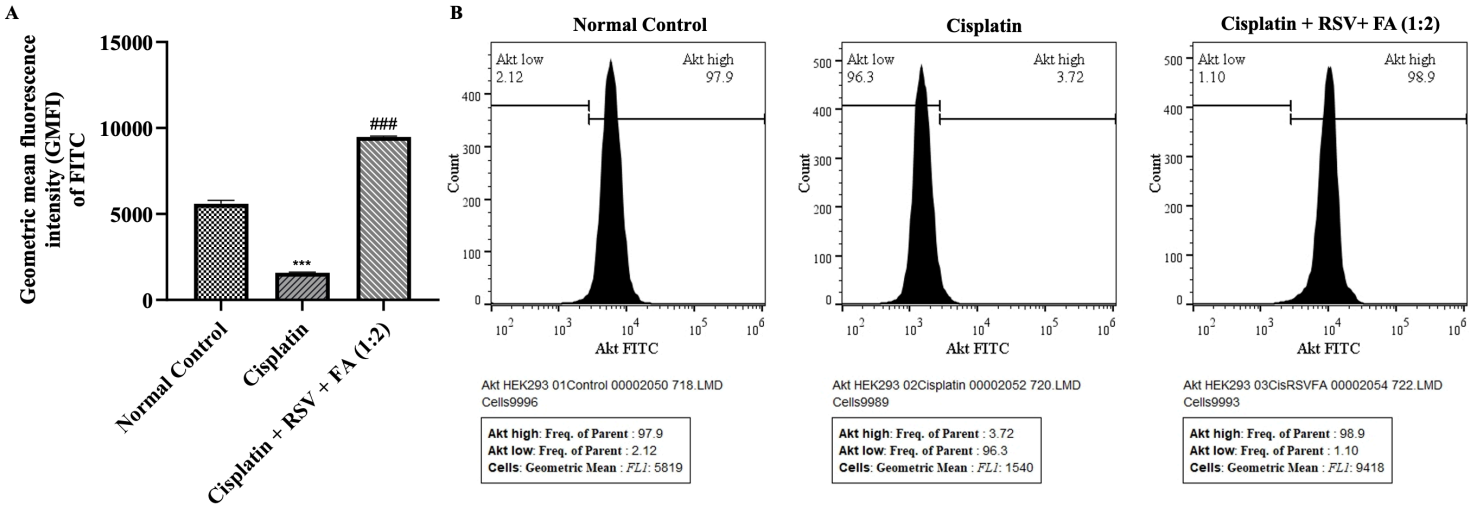

Figure 6

(A) The bar diagram represents the geometric mean fluorescence intensity (GMFI) of Akt expression in the different experimental groups. Values represent mean ± SEM of experiments performed in triplicate; one-way ANOVA followed by Bonferroni test, where $^{***}p < 0.001$ compared to the normal control group and $^{###}p < 0.001$ compared to the cisplatin group. **(B)** Flow cytometry histograms showing Akt expression in HEK 293 cells across the different experimental groups.

Abbreviations: RSV, Resveratrol; FA, Ferulic acid.

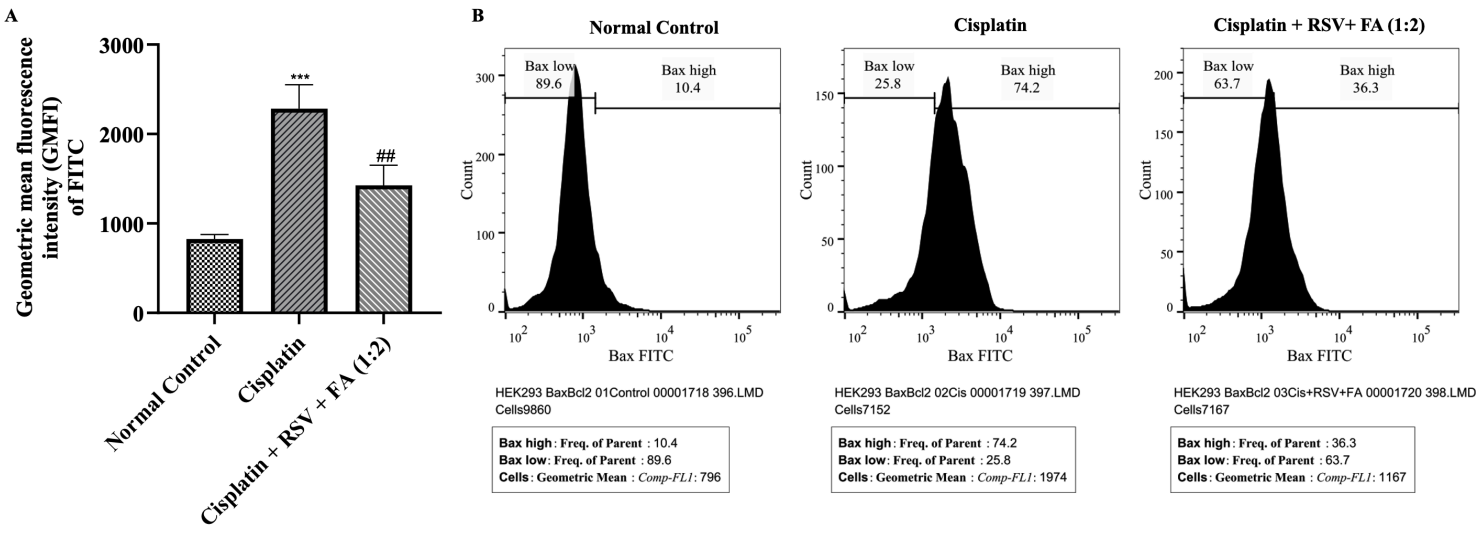

Figure 7

(A) The bar diagram represents the geometric mean fluorescence intensity (GMFI) of Bax expression in the different experimental groups. Values represent mean ± SEM of experiments performed in triplicate; one-way ANOVA followed by Bonferroni test, where $^{***}p < 0.001$ compared to the normal control group

and $^{\#\#}p < 0.01$ compared to the cisplatin group. **(B)** Flow cytometry histograms showing Bax expression in HEK 293 cells across the different experimental groups.

Abbreviations: RSV, Resveratrol; FA, Ferulic acid.

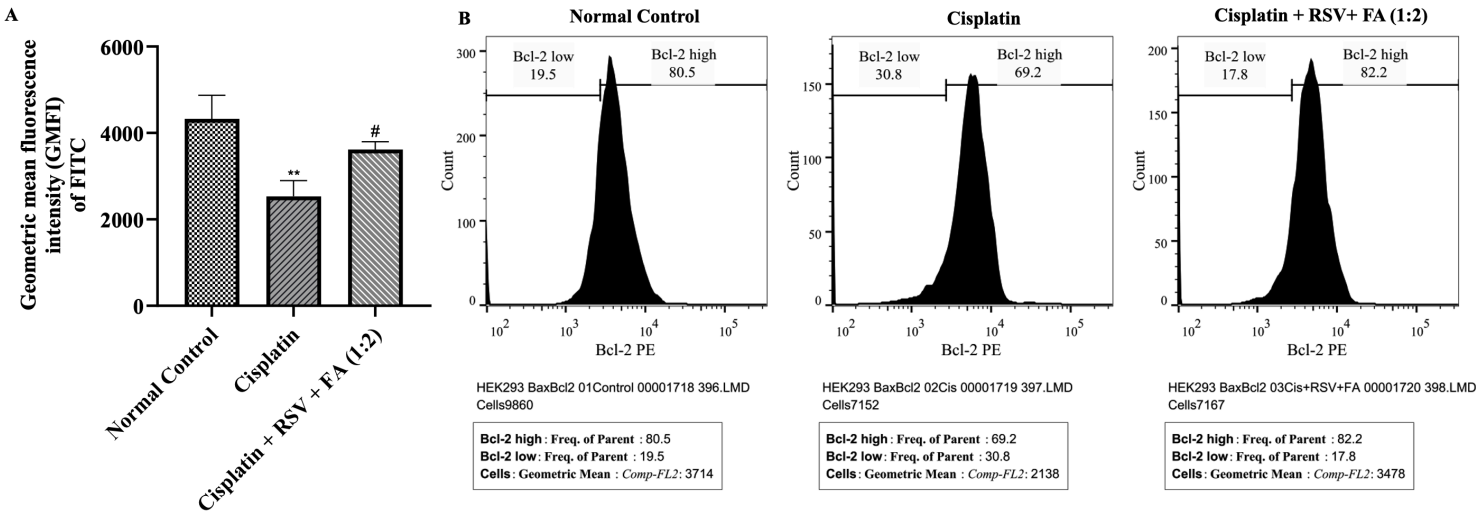

Figure 8

(A) The bar diagram represents the geometric mean fluorescence intensity (GMFI) of Bcl-2 expression in the different experimental groups. Values represent mean ± SEM of experiments performed in triplicate; one-way ANOVA followed by Bonferroni test, where $^{**}p < 0.01$ compared to the normal control group and $^{\#}p < 0.05$ compared to the cisplatin group. **(B)** Flow cytometry histograms showing Bcl-2 expression in HEK 293 cells across the different experimental groups.

Abbreviations: RSV, Resveratrol; FA, Ferulic acid.

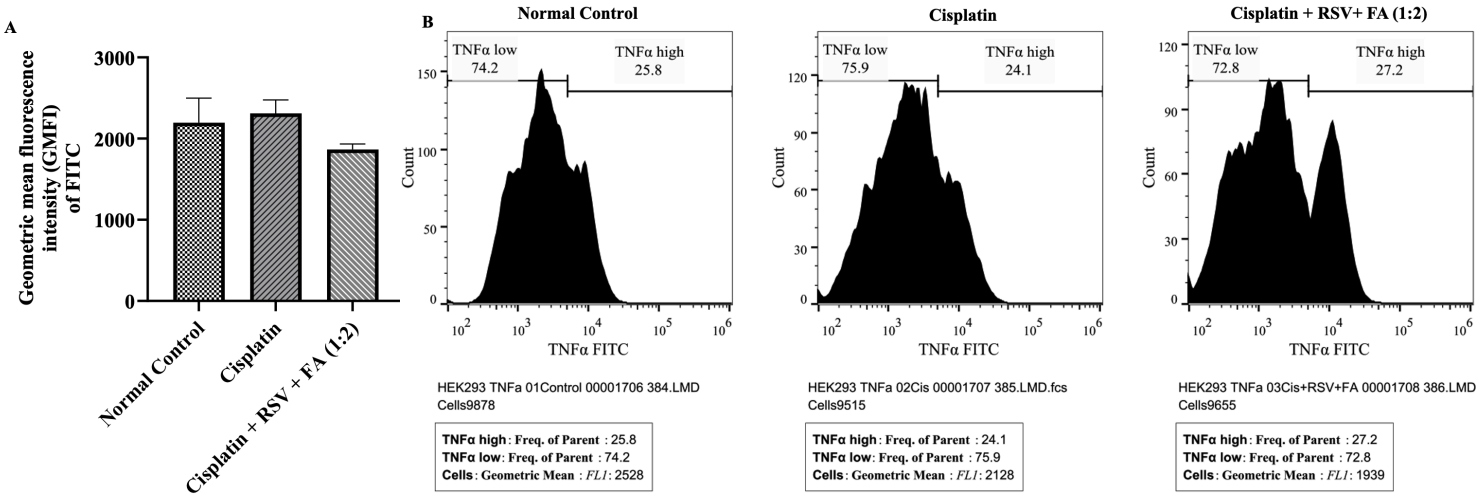

Figure 9

(A) The bar diagram represents the geometric mean fluorescence intensity (GMFI) of TNF-α expression in the different experimental groups. Values represent mean ± SEM of experiments performed in triplicate; one-way ANOVA followed by Bonferroni test, where no significant changes were observed between the groups. **(B)** Flow cytometry histograms showing TNF-α expression in HEK 293 cells across the different experimental groups.

Abbreviations: RSV, Resveratrol; FA, Ferulic acid.

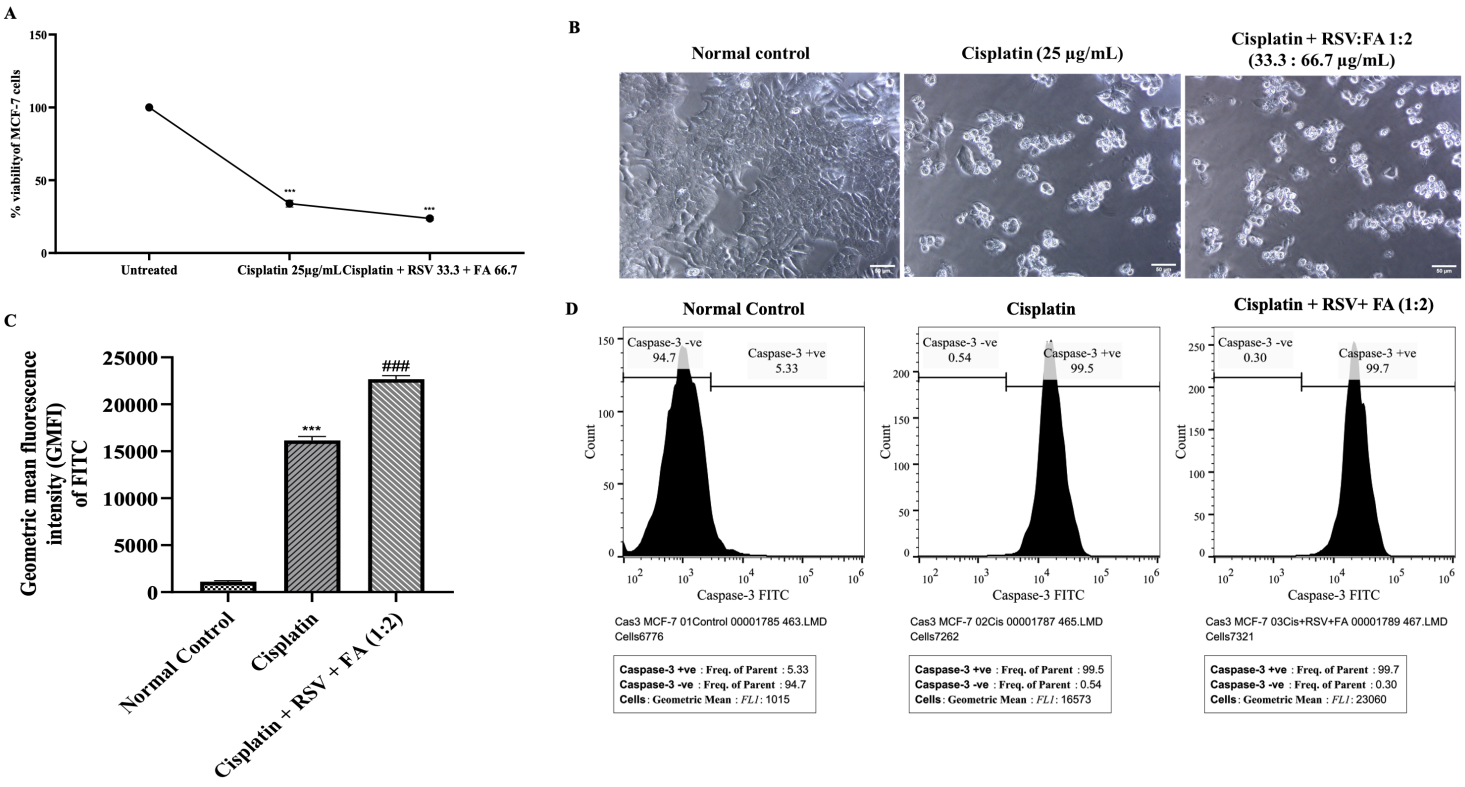

Figure 10

(A) The figure shows the decrease in the percentage viability of MCF-7 cells in different experimental groups. Values represent mean ± SEM of experiments performed in triplicate; one-way ANOVA followed by Bonferroni test, where $^{***}p < 0.001$ compared to the normal control group and $^{###}p < 0.001$ compared to the cisplatin group. **(B)** Cell morphology of MCF-7 cells treated with different concentrations and ratios of cisplatin, resveratrol (RSV), and ferulic acid (FA). The bar scale is 50 µm. **(C)** The bar diagram shows the geometric mean fluorescence intensity (GMFI) of caspase-3 expression across the experimental groups. Values represent mean ± SEM of experiments performed in triplicate; one-way ANOVA followed by Bonferroni test, where $^{***}p < 0.001$ compared to the normal control group and $^{###}p < 0.001$ compared to the cisplatin group. **(D)** Flow cytometry histograms showing caspase-3 expression in MCF-7 cells across the different experimental groups.

Abbreviations: RSV, Resveratrol; FA, Ferulic acid.

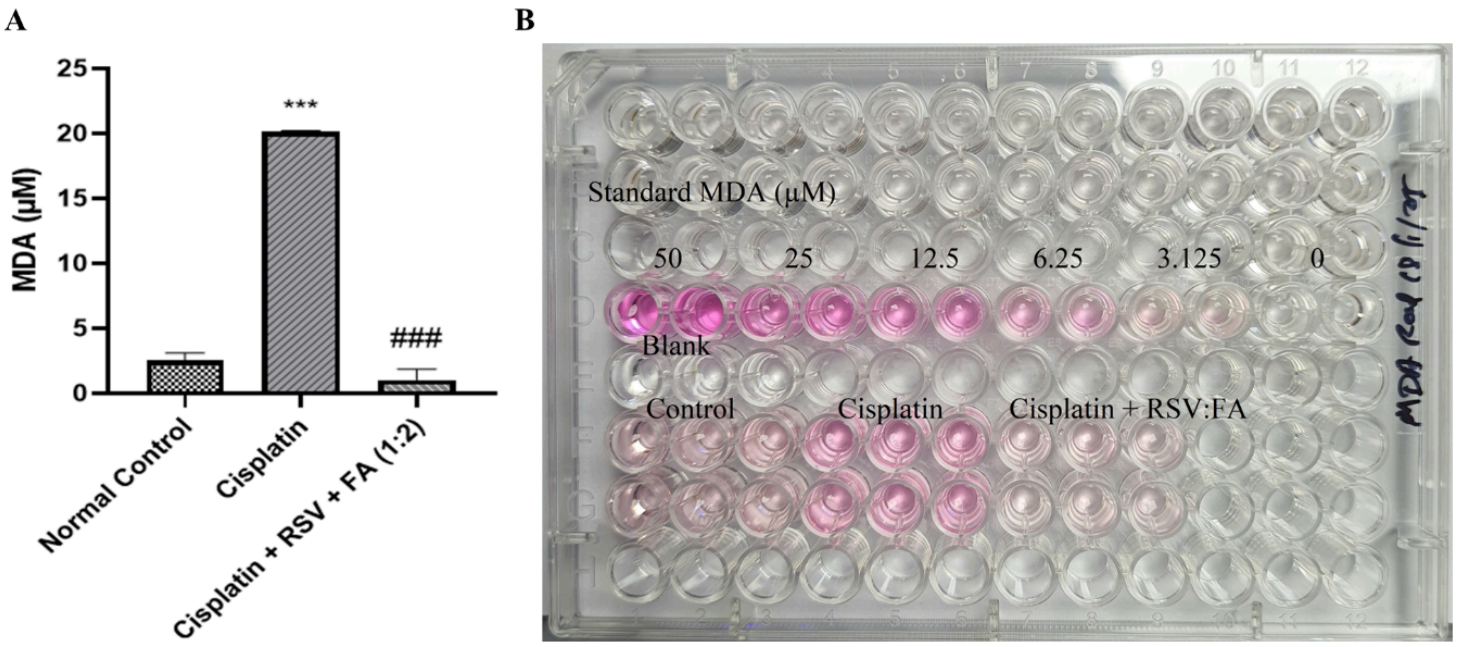

Figure 11

(A) The bar diagram shows the geometric mean fluorescence intensity (GMFI) of MDA across the experimental groups. Values represent mean ± SEM of experiments performed in triplicate; one-way ANOVA followed by Bonferroni test, where $^{***}p < 0.001$ compared to the normal control group and $^{###}p < 0.001$ compared to the cisplatin group. **(B)** MDA estimation using 96-well plates, showing across the different experimental groups.

Abbreviations: RSV, Resveratrol; FA, Ferulic acid.